01 Jul 2013

Microwave Assisted Reconstruction of Optical Interferograms for Distributed Fiber Optic Sensing

Jie Huang
Missouri University of Science and Technology, jieh@mst.edu

Lei Hua

Xinwei Lan

Tao Wei

et. al. For a complete list of authors, see https://scholarsmine.mst.edu/ele_comeng_facwork/3261

Recommended Citation

J. Huang et al., "Microwave Assisted Reconstruction of Optical Interferograms for Distributed Fiber Optic Sensing," *Optics Express*, vol. 21, no. 15, pp. 18152-18159, Optical Society of America, Jul 2013.
The definitive version is available at https://doi.org/10.1364/OE.21.018152

Microwave assisted reconstruction of optical interferograms for distributed fiber optic sensing

Jie Huang,[1] Lei Hua,[1] Xinwei Lan,[1] Tao Wei,[2] and Hai Xiao[1,*]

[1]*Department of Electrical and Computer Engineering, Missouri University of Science and Technology, Rolla, MO 65409, USA*

[2]*Department of Electrical, Computer and Biomedical Engineering, University of Rhode Island, Kingston, RI, 02881, USA*

[*]*xiaoha@mst.edu*

Abstract: This paper reports a distributed fiber optic sensing technique through microwave assisted separation and reconstruction of optical interferograms in spectrum domain. The approach involves sending a microwave-modulated optical signal through cascaded fiber optic interferometers. The microwave signal was used to resolve the position and reflectivity of each sensor along the optical fiber. By sweeping the optical wavelength and detecting the modulation signal, the optical spectrum of each sensor can be reconstructed. Three cascaded fiber optic extrinsic Fabry-Perot interferometric sensors were used to prove the concept. Their microwave-reconstructed interferogram matched well with those recorded individually using an optical spectrum analyzer. The application in distributed strain measurement has also been demonstrated.

OCIS codes: (060.2370) Fiber optics sensors; (060.4230) Multiplexing; (120.3180) Interferometry.

References and links

1. M. LeBlanc, S. Y. Huang, M. Ohn, R. M. Measures, A. Guemes, and A. Othonos, "Distributed strain measurement based on a fiber Bragg grating and its reflection spectrum analysis," Opt. Lett. **21**(17), 1405–1407 (1996).
2. W. Wang, J. Gong, B. Dong, D. Y. Wang, T. J. Shillig, and A. Wang, "A large serial time-division multiplexed fiber Bragg grating sensor network," J. Lightwave Technol. **30**(17), 2751–2756 (2012).
3. Z. Zhang and X. Bao, "Distributed optical fiber vibration sensor based on spectrum analysis of Polarization-OTDR system," Opt. Express **16**(14), 10240–10247 (2008).
4. Y. Dong, L. Chen, and X. Bao, "Time-division multiplexing-based BOTDA over 100 km sensing length," Opt. Lett. **36**(2), 277–279 (2011).
5. W. Eickhoff and R. Ulrich, "Optical frequency domain reflectometry in single-mode fiber," Appl. Phys. Lett. **39**(9), 693–695 (1981).
6. R. Passy, N. Gisin, J.-P. von der Weid, and H. Gilgen, "Experimental and theoretical investigations of coherent OFDR with semiconductor laser sources," J. Lightwave Technol. **12**(9), 1622–1630 (1994).
7. T. Zhu, D. Wu, M. Liu, and D.-W. Duan, "In-line fiber optic interferometric sensors in single-mode fibers," Sensors (Basel) **12**(12), 10430–10449 (2012).
8. J. Wang, B. Dong, E. Lally, J. Gong, M. Han, and A. Wang, "Multiplexed high temperature sensing with sapphire fiber air gap-based extrinsic Fabry-Perot interferometers," Opt. Lett. **35**(5), 619–621 (2010).
9. X. Li, Q. Sun, D. Liu, R. Liang, J. Zhang, J. Wo, P. P. Shum, and D. Liu, "Simultaneous wavelength and frequency encoded microstructure based quasi-distributed temperature sensor," Opt. Express **20**(11), 12076–12084 (2012).

1. Introduction

With many advantages such as small size, light weight, immunity to electromagnetic interference, high sensitivity, and resistance to corrosion, fiber optic sensors have found broad applications in various fields. Given the very small loss of light transmission in an optical fiber, it is also believed that optical fiber sensors have the unique advantage of distributed sensing. In general, spatially distributed information can be acquired by either multiplexing a large number of discrete sensors or by sending a pulsed signal to probe the spatially resolved information as a function of time-of-arrival.

In multiplexed sensing, many sensors can be trained in series on an optical fiber to sample the spatially distributed information. These cascaded sensors have their unique signatures that can be unambiguously identified. For example, a number of fiber Bragg gratings (FBGs) can be cascaded along an optical fiber and uniquely identified by their different resonant wavelengths in spectrum domain [1]. However, the maximum number of FBG sensors multiplexed along a fiber is limited by the bandwidth of the light source and the required frequency interval per sensor for prevention of overlapped signals and crosstalks. Recently, a wavelength scanning, time division multiplexing method has been demonstrated to interrogate 1000 ultraweak FBGs for distributed temperature sensing [2]. However, the time domain signal was noisy and multiple measurements were required to achieve an acceptable signal-to-noise ratio (SNR).

Another technique, known as the time domain reflectometry (TDR), has also been widely explored for spatially continues sensing of various parameters [3]. In TDR, a pulsed signal is sent along a fiber and the time/space resolved reflections are collected and analyzed. The reflections can be from Rayleigh, Brillouin and Raman scatterings. For example, a long-range spatially continuous Brillouin optical time-domain analysis (BOTDA) measurement system has been demonstrated with a spatial resolution of 2m over a span of 100km [4]. The advantages of TDR include long span of coverage and spatial continuity. However, the measurement resolution of TDR is generally low due to the inherently weak scatterings.

To improve the SNR and the spatial resolution of TDR, optical frequency domain reflectometry (OFDR) has been proposed [5]. In OFDR, a frequency-scanning, highly coherent source and a Michelson interferometer are used to encode the time-of-arrival information into frequency domain signals, which can be Fourier-transformed back to time/space domain. The SNR and spatial resolution of OFDR are noticeably higher than the traditional TDR method. However, the measurement accuracy has been limited by the power fluctuations and/or random changes in polarizations. In addition, the measurement distance of OFDR is on the order of several hundred meters due to the availability of high-quality light sources with both long coherence length and fine frequency scanning intervals [6].

Among many types of sensors, fiber optic interferometers are known for their high resolution and design flexibility for measurement of various physical, chemical and biological parameters [7]. One can imagine that multiplexed fiber optic interferometers would have broad applications in many fields. Multiplexing several fiber interferometers has been demonstrated in wavelength domain by designing large differences in their initial optical path differences (OPD). As such, the superimposed spectral interferogram can be separated by frequency analysis [8, 9], e.g., by Fourier transform. However, the number of sensors to be multiplexed is limited by the spectral width of the light source as well as the differences in OPD.

In this paper, we report a new method to multiplex fiber optic interferometers for distributed sensing through microwave assisted separation and reconstruction of optical interferograms in spectrum domain. Cascaded fiber optic extrinsic Fabry-Perot interferometers (EFPI) sensors are used for the purpose of demonstration. It is expected that the proposed technique can also be used for multiplexing other types of fiber interferometers.

2. Microwave assisted multiplexing of interferometric sensors

The proposed approach is schematically shown in Fig. 1. The light from a broadband source is launched into a tunable optical filter and then intensity-modulated by a microwave signal whose modulation frequency can be scanned via computer control. The intensity of the microwave modulated light can be expressed as:

$$I = I_0\left[1 + M\cos\left(\omega t\right)\right] \quad (1)$$

#190439 - $15.00 USD Received 13 May 2013; revised 19 Jun 2013; accepted 9 Jul 2013; published 22 Jul 2013

where I_0 is the intensity of the light source, M is the modulation depth, and ω is the frequency of the microwave signal.

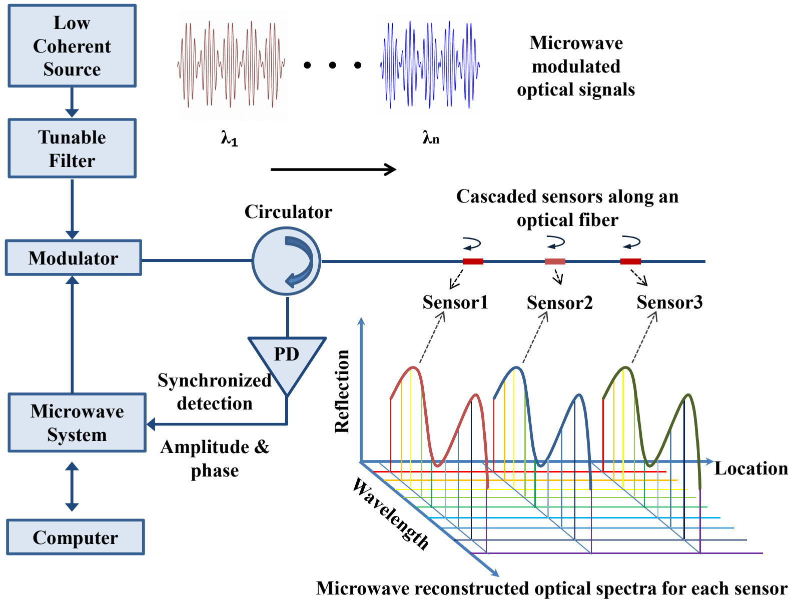

Fig. 1. Schematic illustration of the microwave assisted multiplexing of fiber optic interferometric sensors. PD: photo-detector

The microwave-modulated light, where the optical is the carrier and the microwave is the envelope, is then sent into an optical fiber with cascaded reflective EFPI sensors through a fiber optic circulator. The reflection of each EFPI sensor can be designed to be weak enough so that the light can be transmitted over many sensors and the multiple reflections within each sensor is negligible. The coherence length of the light, which is determined by the bandwidth of the tunable filter, is much larger than the optical path differences (OPD) of the EFPI sensors but much smaller than the distance between two adjacent sensors. As a result, optical interference occurs within one sensor while the optical interference between sensors is avoided. The optical interference signal Γ_j of the j-th EFPI can be written as:

$$\Gamma_j = I_0\left[1 + M\cos\left(\omega(t+\tau_j)\right)\right]R_j \tag{2}$$

and

$$R_j(\lambda_m) = R_{j1} + R_{j2} + 2\sqrt{R_{j1}R_{j2}}\cos\left(\frac{2\pi}{\lambda_m}\cdot OPD_j + \phi_j\right) \tag{3}$$

where $R_j(\lambda_m)$ is the optical interference signal; R_{j1} and R_{j2} are the optical reflectivity of the two endfaces of the cavity, respectively; λ_m is the optical wavelength set by the optical tunable filter; OPD_j is the optical path difference; ϕ_j is the initial phase; τ_j is the propagation delay of the microwave envelope of the j-th EFPI, which can be calculated using the following equation,

$$\tau_j = \frac{2D_j}{v} \tag{4}$$

where D_j is approximately the distance between the j-th sensor and the photodetector (PD), v is the group velocity of the microwave-modulated light transmitted inside the optical fiber.

#190439 - $15.00 USD Received 13 May 2013; revised 19 Jun 2013; accepted 9 Jul 2013; published 22 Jul 2013

The optical interference signals of the sensors travel backwards, pass the fiber circulator and are detected by a high-speed photodetector. The optical signal is the superposition of all the cascaded EFPIs, given by,

$$Y = \sum_{j=1}^{N} \Gamma_j = \sum_{j=1}^{N} I_0 R_j \left[1 + M \cos\left(\omega (t + \tau_j) \right) \right] \tag{5}$$

where N is the total number of EFPIs cascaded along the fiber.

The optical detection is synchronized with the microwave modulation frequency (ω) so that the amplitude and the phase of the AC term (i.e., the cos(ωt) term in Eq. (5) are obtained. After scanning the microwave frequency through the entire available range, the complex microwave reflection spectrum (with both amplitude and phase) is obtained. By applying a complex and inverse Fourier-transform to the microwave spectrum, a series of delta functions are obtained at discrete time positions, given by:

$$y_j = AMI_0 R_j \quad at \quad t = \tau_j \text{ and } j = 1, 2, ...N \tag{6}$$

where A is the gain of the microwave detection.

As indicated in Eq. (6), the discrete time domain signals are proportional to the optical interference signals (R_j) of the cascaded EFPI sensors at a particular optical wavelength (λ_m) determined by the tunable filter. In addition, Eq. (6) also provides the locations of the sensors along the optical fiber because it has nonzero values only at the specific propagation delays (τ_j) corresponding to the sensor locations (D_j) as given by Eq. (4).

By sweeping the optical wavelength and repeating the microwave measurement, we can obtain the discrete optical interference signals (separated in the time domain) at different wavelengths. These data points can then be used to construct the optical interferograms of the cascaded EFPI sensors.

3. System realization and concept demonstration

Figure 2 shows an example system to verify the proposed concept. The broadband light source used was an amplified spontaneous emission (ASE) source emitting in the spectrum of 1530-1560nm. The tunable filter had a full width at half maxima (FWHM) of about 1nm, corresponding to a coherence length of about 1 mm. The intensity modulation of the bandpass filtered light was performed through an electro-optic modulator (EOM). An optical polarizer and an optical polarization controller are placed before the EOM to enhance the modulation efficiency. The microwave source and detection were realized through a vector network analyzer (VNA). The EOM was driven by the output from the Port 1 (P1) of the VNA. The microwave signal from VNA was amplified to obtain a desirable modulation index. The modulated light was then routed to the cascaded EFPI sensors via an optical circulator. By fine tuning the polarization controller and the driving power to the EOM, we obtained a modulation index of 100% at 3GHz.

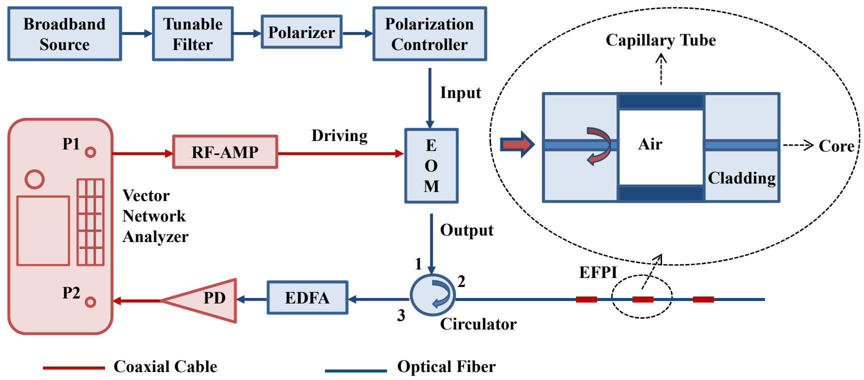

Fig. 2. Schematic of the system configuration and implementation for concept demonstration. RF-AMP: radio frequency-amplifier, EOM: electro-optic modulator, EDFA: Erbium-doped fiber amplifier, PD: photo-detector, EFPI: extrinsic Fabry-Perot interferometer, P1/P2: Port 1/Port 2

The reflected signals from the EFPIs were first amplified by an EDFA and then received by a high speed photo-detector (100 MHz to 6 GHz), which was connected to the Port 2 (P2) of the VNA. To further improve the signal quality, a microwave amplifier could be placed after the photodetector to amplify the converted microwave analog signal. By sweeping the modulation frequency of the VNA, the amplitude and phase information of the received microwave signals (i.e., the scattering parameter S_{21} of the VNA) were recorded to reconstruct the microwave spectrum.

For the purpose of concept demonstration, three EFPI sensors were used. The EFPIs were made by fusion-splicing a capillary tube between two singlemode fibers, with cavity lengths of approximately 80, 70, and 140 μm, respectively. They were separated by a distance of about 100 mm apart along a single mode fiber. The intermediate frequency bandwidth (IFBW) of the VNA was set to 300 Hz. The microwave power at Port 1 of VNA was set to −11 dBm and pre-amplified to 27 dBm for all frequency range to drive the EOM.

By scanning the microwave frequency from 100 MHz to 6 GHz with 1601 sampling points and recording their amplitude and phase information from Port 2 of VNA, the microwave reflection spectrum (S_{21}) was obtained. After applying a complex and inverse Fourier transform, the time-resolved discrete reflections of the three EFPIs were obtained. The tunable filter was then scanned from 1545 to 1560 nm with an interval of 0.5 nm. The whole procedure took about 1 minute, which included the time required for the VNA to scan through the entire available frequency span, data acquisition, signal analysis, stepping the wavelength of the tunable filter through the spectrum range, and interferogram reconstruction.

#190439 - $15.00 USD Received 13 May 2013; revised 19 Jun 2013; accepted 9 Jul 2013; published 22 Jul 2013

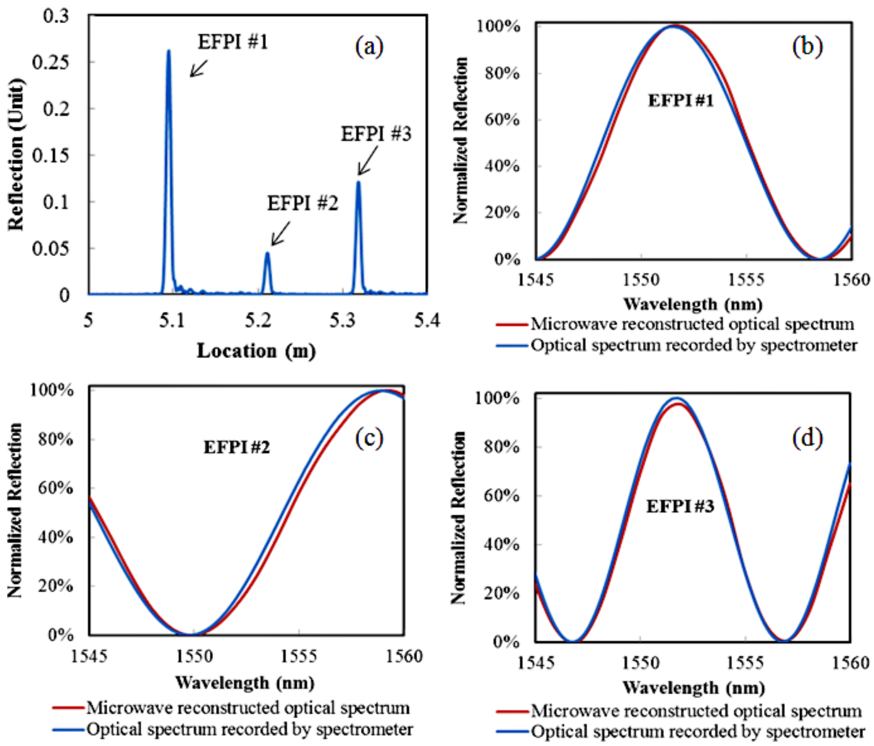

Fig. 3. (a) Time domain signal after applying a complex inverse Fourier transform to the microwave spectrum with the center wavelength of the tunable filter set to be 1552 nm, (b), (c) and (d) Normalized microwave-reconstructed optical interferograms of the three EFPIs in comparison with their spectra measured individually using an OSA, respectively.

Figure 3(a) plots the time-resolved discrete reflections where the optical carrier wavelength was tuned to 1552 nm. Three reflections (three EFPIs) can be clearly observed in time domain with good signal-to-noise ratio. Although the two air/glass interfaces in each capillary tube had two optical reflections, they could not be resolved in microwave domain due to the large wavelength of microwave comparing with the cavity lengths of the EFPIs. The observed microwave reflections is proportional to the total optical reflection of the EFPI structure, which was a result of optical interference when the coherence length of the light source was much large than the cavity length. The distance between two consecutive EFPIs was far larger than the coherence length of the input light source so that there was no interference between two EFPIs.

Figures 3(b)–3(d) plot the reconstructed optical interferograms of the three EFPIs, respectively. The red curves represent the microwave reconstructed optical interferograms, and the blue curves are the interference spectra recorded individually using an optical spectrum analyzer (OSA). The microwave intensities were all normalized based on their corresponding optical intensities for comparison. The reconstructed optical interferograms matched well with those measured by the OSA. We believe that the difference is mainly resulted from the uneven gain spectrum of the EDFA used in the experiments.

4. Demonstration of distributed sensing

To demonstrate the proposed method for distributed sensing, a strain test was performed. The axial strain was applied to the second EFPI while the other two sensors were relaxed. The two ends of the second EFPI sensor were tightly attached to a motorized translation stage and a fixed stage using all-purpose glue, respectively. The length between two attaching points was precisely measured to be 100 mm. The interferograms of the three EFPIs were recorded using the microwave method as the distance between the two points was increased step by step. The distance was increased at a step of 5 μm, corresponding to a strain increment of 50 με per step.

By applying the 4th order polynomial curve-fitting to all the reconstructed spectra and monitoring the center wavelength of the interference valleys, the wavelength shift of each sensor was plotted as a function of the axial strain. Figure 4(a) shows the 3D plot of the spectral shift of the three multiplexed EFPIs along the optical fiber as a function of the applied strain. The second sensor had an obvious response to the applied strain while the other sensors had no responses, indicating that the proposed distributed sensing method had little crosstalk among sensors. Figure 4(b) plots the second sensor in response to the applied axial strain, where the wavelength shift of the interferogram increases linearly as a function of the applied strain with a slope of 0.0024 nm/με. The inset of Fig. 4(b) plots a few examples of reconstructed spectra as the applied strain increased. The increasing strain did not incur noticeable loss in the reflection spectra. The spectra of the other two sensors had no any observable shift.

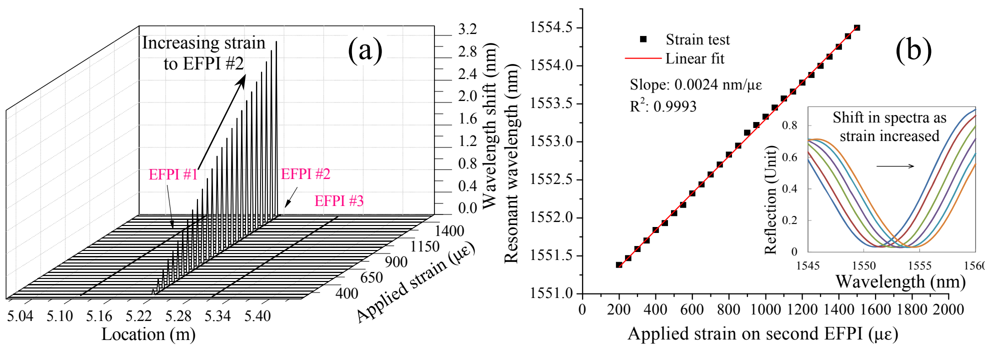

Fig. 4. (a) Distributed strain measurement using three multiplexed EFPI sensors, where strain is applied on EFPI #2 only, (b) Interferogram shift of the EFPI #2 as a function of applied axial strain. Inset: Interferograms of EFPI #2 at various applied strains.

The spatial resolution ΔD_{min} (i.e., the minimum distance between two adjacent sensors) is determined by the microwave frequency bandwidth according to the following equation,

$$\Delta D_{\min} = \frac{1}{2B_{RF}} v \tag{7}$$

where B_{RF} is the bandwidth (i.e., the maximum scanning frequency range) of the microwave source. A larger bandwidth results in a better spatial resolution. For example, if the bandwidth of the microwave source is 6GHz, the minimum distance between two adjacent sensors is about 1.7cm. Of course as stated earlier, the separation between two sensors needs to be significantly larger than the coherence length of the spectrally filtered optical source to avoid the optical interference between two adjacent sensors.

Because the cascaded EFPIs are uniquely identified in the microwave domain, they can be made to have the same OPD. On contrast, the typical optical spectral domain Fourier transform based multiplexing method [8, 9] requires the multiplexed sensors to have significantly different OPDs. The maximum number of sensors can be multiplexed depends on the insertion loss (including reflection) of each sensor, the dynamic range of the microwave instrument, and the dynamic range of the photodetector. In general, the cascaded EFPIs can be made to have weak reflectivity to reduce the insertion loss. The optical signals can be further amplified by using EDFAs. It is expected that the reported microwave method is able to multiplex much more interferometers than the typical optical spectral domain Fourier transform based multiplexing method.

#190439 - $15.00 USD Received 13 May 2013; revised 19 Jun 2013; accepted 9 Jul 2013; published 22 Jul 2013

5. Conclusion

To summarize, a microwave based method was studied for multiplexing fiber optic interferometers for distributed sensing. By sending a microwave-modulated optical signal through cascaded fiber optic interferometers, the microwave signals are used to resolve the position and reflectivity of each sensor along the optical fiber. The coherence length of the optical source is chosen to be larger than the optical path differences of the cascaded interferometers but smaller than the spatial separation between sensors. As such, the cascaded interferometers can be uniquely identified by complex Fourier transform of the microwave spectrum. By sweeping the optical wavelength, the optical spectrum of each sensor can be reconstructed. Three cascaded EFPIs along an optical fiber were used to demonstrate the concept. The optical interferograms of the EFPIs were reconstructed unambiguously and they matched well with those measured individually using an OSA. Distributed strain sensing was conducted to prove the system's effectiveness in sensing applications. It is necessary to note that although three EFPIs are used for the purpose of concept demonstration, other types of fiber interferometric sensors can also be implemented using the method. The reported microwave method can multiplex interferometric sensors with the same OPDs. In comparison with the traditional optical spectral domain Fourier transform based multiplexing approach, the reported method has the advantages of multiplexing much more sensors because it is not limited by the bandwidth of the optical source. It is expected that the proposed multiplexing technique may find many applications for distributed measurement of various physical, chemical and biological parameters.

Acknowledgment

The research work was supported by the National Science Foundation under the contract CMMI-1200787.

#190439 - $15.00 USD Received 13 May 2013; revised 19 Jun 2013; accepted 9 Jul 2013; published 22 Jul 2013